Axial compressive behavior of CFRP reinforced concrete filled steel tube short columns with a circumferential gap

Binglun Chen[1],Zhishuo Yang*[2]

[1]China MCC5 Group Corp., Ltd, ChengDu 610036, Si Chuan Province, China
[2] School of Civil Engineering, Jiaying University, Meizhou 514015, Guangdong Province, China

Abstract: Carbon fiber reinforced polymer (Carbon Reinforced Polymer Plastic) can effectively use its own tensile properties to provide stronger restraint for concrete, and can delay the buckling of steel pipes after yielding, and has been widely used in engineering repair and reinforcement. For the CFST composite structure with annular void defects, whether the reinforcement of CFRP can make up for a series of problems caused by void defects is still a fog. In order to explore the axial compression performance of CFRP (carbon fiber cloth) reinforced concrete-filled steel tubular short columns with circumferential void defects, 12 CFRP-reinforced CFRP short columns with circumferential void defects were proposed to be reinforced with a void ratio of 1.1-2.2%. The axial compression performance test was carried out to analyze the influence of parameters such as void ratio and the number of reinforcement layers on the axial compression performance, and a corresponding finite element model was established to assist in analyzing its working mechanism. The test results show that with the increase of the void ratio, the ultimate bearing capacity and the corresponding displacement of the components show a downward trend, and the deformation capacity is also greatly weakened. The ductility of the empty specimen is significantly improved, and the ductility of the specimen is also strengthened. With the increase of the number of reinforcement layers, the buckling deformation restraint effect of CFRP on the steel pipe becomes more and more significant, and it also provides better hoop restraint for the core concrete. To a certain extent, CFRP can reduce the effect of annular voiding defects.

1 Introduction

CFST is widely used in practical projects such as high-rise buildings and bridges because of its high bearing capacity, good plasticity, toughness and seismic performance, and convenient construction[1-3].However, in the actual use of the structure, it is often accompanied by a certain degree of defects (such as geometric defects in the processing of steel pipes, defects in the concrete pouring process, etc.). A large number of test results for CFST composite structures show that most of them have voiding defects[4], especially for vertical bearing CFST components (such as CFST columns, bridge piers, etc.), the core concrete occurs during its service life cycle. When the shrinkage, creep, or the large temperature difference between the steel pipe and the concrete leads to a difference in the expansion and deformation between the two, the component is more prone to the annular void defect[5-7], as shown in Figure 1. On the one hand, the existence of the hoop void defect not only weakens the interaction between the two, but also greatly weakens the confinement effect of the steel tube on the core concrete, thereby reducing the plasticity and compressive strength of the core concrete. On the other hand, the supporting effect of the core concrete on the steel pipe is weakened, and the steel pipe is partially buckled, resulting in a decrease in the mechanical properties such as the bearing capacity, ductility, and stiffness of the components, which poses a great safety hazard to the actual structure.

Although the engineering and academic circles have carried out numerous explorations on how to deal with the impact of repairing the hoop void defect on the overall structure, no unified standard has been formed, and the conventional treatment methods (such as grouting) for the hoop void problem have not been formed. The influence of such defects cannot be completely eliminated[8]. In recent years, new fiber reinforced composite materials (CFRP) have gradually attracted the attention of scholars due to their unique material performance advantages, and have been widely used in structural reconstruction and reinforcement projects[9-10]. Kabir[[11] firstly confirmed that the presence of CFRP can significantly improve the stability of the specimen by the experimental study of the CFRP-reinforced damaged area of the steel tube column. At the same time, Wang[12] used CFRP to strengthen the damaged steel plate and found that the existence of CFRP not only effectively delayed the fatigue life of the steel plate, but also had a better reinforcement effect on the edge-cracked steel plate than the central cracked specimen. Gu Wei[13] introduced in detail the working mechanism of CFRP-constrained CFST columns under axial

Binglun Chen, Email: 1043872577@qq.com.
Zhishuo Yang, Email: chengbinglun@163.com.

compression. Sundarraja[14], Prabhu[15]and others found through experimental research that the increase of the number of CFRP layers and the reduction of the spacing can significantly improve the bearing capacity and deformation capacity, and the use of hoop reinforcement can better delay the deformation of the steel pipe. In addition, Wang Qingli, Wang Chunyu, Ding Lei et al[16-18] found that when the slenderness ratio is the same, the ultimate bearing capacity decreases with the increase of the eccentricity; when the eccentricity is the same, with the increase of the slenderness ratio, the ultimate bearing capacity When the eccentricity is not considered (the eccentricity is 0, that is, the axial pressure), as the slenderness ratio increases, the constraint effect on the middle of the column is weakened; in terms of bearing capacity, as the slenderness ratio increases, the column The peak load of CFRP-reinforced columns showed a decreasing trend, and the peak load of CFRP-reinforced columns decreased slightly. Regarding the seismic performance of the reinforced concrete-filled steel tubular structure, Qin and Xiao[19] believed that CFRP can effectively constrain the failure form of the column and significantly improve the energy dissipation capacity of the specimen. Tao et al[20] used CFRP to strengthen the CFST column under fire damage and found that the ultimate lateral strength, bending stiffness, energy dissipation and ductility of the components were greatly improved. Zhang Daijun et al[21] also studied the change of mechanical properties of CFRP reinforced concrete-filled steel tubes under the condition of long-term natural aging.

At present, the relevant researches that have been carried out mainly focus on the use of CFRP to strengthen circular, rectangular concrete columns and CFST columns, while the relevant research on the use of CFRP to strengthen CFST members with circumferential void defects is rarely reported. For this reason, in this paper, the axial compression test of CFRP-reinforced concrete-filled steel tubular short columns with hoop void defect is carried out with the changing parameters of the number of CFRP-reinforced layers and the void ratio. By comparing the development of bearing capacity and failure form of CFRP short columns with hoop void defects under two void ratios with different CFRP reinforcement layers, and establishing an effective finite element model for auxiliary analysis, it is further revealed that Influence mechanism of CFRP strengthening of concrete-filled steel tubular specimens with hoop void defect.

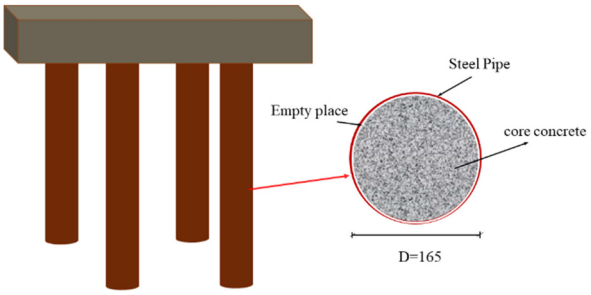

Fig.1 Circumferential gap Diagram of component

2 Trial overview

2.1 Experiment material

The outer steel pipes of the components are made of Q235 straight seam steel pipes, the core concrete is C60 high-grade concrete, and the CFRP is made of Japanese Toray fiber cloth, the model is UT70-30. The concrete mix ratios are shown in Table 1. According to《Room Temperature Tensile Test Method for Metallic Materials》 (GB/T228-2010)[22], 《Standard for Test Method for Mechanical Properties of Ordinary Concrete》 (GB/T50081-2002)[23] and 《Oriented Fiber Reinforced Polymer Matrix Composites Tensile Properties Test Methods》 (GB/T3354-2014)[24], the tensile and compressive properties of steel pipes, CFRP and concrete were tested, respectively, and the properties of the properties are listed in Tables 2, 3, and 4, respectively.

Table 1 Mix proportion of concrete

Concrete type	water	sand	cement	fly ash	stone	water reducer
C60	190.0	770.0	425.0	170.0	775.0	6.5

Table 2 Material properties of steel

Numbering	f_y /Mpa	ε_y / $\mu\varepsilon$	f_u /Mpa	E_s /Gpa	V	δ /%
1	320.2	2127.34	385.0	183.8	0.274	20.9
2	300.5	2173.37	358.2	185.1	0.271	21.2
3	310.1	2266.67	375.4	191.4	0.278	21.1
mean	310.3	2189.13	372.9	186.8	0.274	21.1

Table 3 Mechanical performance index of CFRP

Paste layers	T/mm	E_f /Mpa	f_{tk} /Mpa	ultimate strain / ε / $\mu\varepsilon$
one	0.17	2.8×105	3602.90	12541.00
two	0.34	2.8×105	3602.90	-

Table 4 Mechanical performance index of concrete

concrete type	slump /mm	Expansion /mm	28d f_{cu} /Mpa	During the test $f_{cu.t}$ /Mpa	E_c /Mpa	Poisson's ratio
C60	280.0	590-600	48.3	57.3	33508.2	0.2

2.2 Test piece production

In this paper, a total of 6 groups of 12 specimens and 2 pre-experimental components without voids are designed. Each group is designed with two specimens with the same parameters. The test parameters mainly include: void ratio and CFRP reinforcement layers. The length L of the test piece is 510mm, the outer diameter D of the section is 165mm, t is the wall thickness of the steel pipe, χ is the void ratio[30], and the information and number of the test piece are shown in Table 5.

Table 5 Main parameters of specimens

Numbering	$L\times D\times t$ / mm	f_{cu} / Mpa	$f_{cu,t}$ / Mpa	f_y / Mpa	layers	missing value /mm	void rate / χ / %
C0-0-0a	510×165×4	48.3	57.3	310.3	-	-	-
C0-0-0b	510×165×4	48.3	57.3	310.3	-	-	-
CC-1-0a	510×165×4	48.3	57.3	310.3	0	0.924	1.1
CC-1-0b	510×165×4	48.3	57.3	310.3	0	0.924	1.1
CC-1-1a	510×165×4	48.3	57.3	310.3	1	0.924	1.1
CC-1-1b	510×165×4	48.3	57.3	310.3	1	0.924	1.1
CC-1-2a	510×165×4	48.3	57.3	310.3	2	0.924	1.1
CC-1-2b	510×165×4	48.3	57.3	310.3	2	0.924	1.1
CC-2-0a	510×165×4	48.3	57.3	310.3	0	1.848	2.2
CC-2-0b	510×165×4	48.3	57.3	310.3	0	1.848	2.2
CC-2-1a	510×165×4	48.3	57.3	310.3	1	1.848	2.2
CC-2-1b	510×165×4	48.3	57.3	310.3	1	1.848	2.2
CC-2-2a	510×165×4	48.3	57.3	310.3	2	1.848	2.2
CC-2-2b	510×165×4	48.3	57.3	310.3	2	1.848	2.2

Note: D is the outer diameter of the section of the CFST member with defects; L is the length of the specimen; t is the wall thickness of the steel pipe; χ [30] is void rate, For annular breakout: χ =(2h)/D ; f_{cu} is concrete strength at 28 days; $f_{cu,t}$ is concrete strength at test time; f_y is steel tube yield strength.

In the process of component preparation, the cutting part of the steel pipe is ground in advance, the lower end plate of the steel pipe is welded with studs[25], the inner and outer sides of the annular iron tube are coated with Vaseline, and longitudinally wrapped with plastic wrap, the outside of the plastic film is coated with Vaseline[29], and the concrete is cured for 12 hours. After that, the annular iron sheet tube is pulled out to form an annular void defect. as shown in picture 2.

CFRP reinforcement is carried out in accordance with the 《Technical Specifications for Reinforcement and Repair of Concrete Structures by Carbon Fiber Sheets》(2007)[26] and the instructions for use of the product. Since the length of the specimen is 510mm and the width of CFRP is 500mm, only the circumferential wrapping length is considered when cutting. After wrapping, the colloid can be completely cured. as shown in Fig.2.

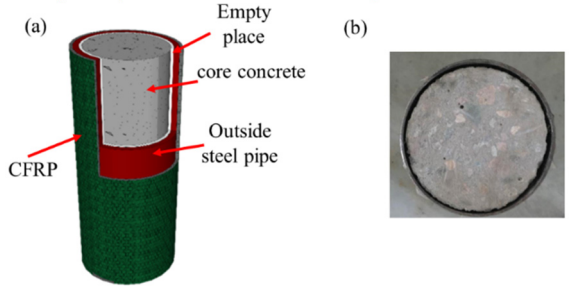

Fig.2 Circumferential gap Specimen Cross section

2.3 Loading device

The tests were all loaded with flat plates, and the loading device was shown in Figure 3. Test loading is divided into preloading and formal loading. All specimens were preloaded in order to physically align the specimens. The preload rate is 1kN/s, and the preload load is 10% of the estimated limit load. When the set load is reached, the press remains in a load-holding state. During the loading process, the numerical changes of the longitudinal strain gauges were continuously observed. When the error of the four strain gauges was small, the specimen was considered to be in the state of axial compression. Otherwise continue with physical alignment. The force-displacement hybrid loading method is adopted for formal loading, and the force-controlled method is adopted in the elastic stage. The loading rate is 1kN/s, the load of each stage is 10% of the estimated limit load, and the load holding time of each stage is 2 minutes; the elastic-plastic stage is entered. The displacement control method was adopted, the loading rate was 0.75 mm/min, and the specimen was continuously loaded until the axial displacement reached 50 mm, and the loading was stopped.

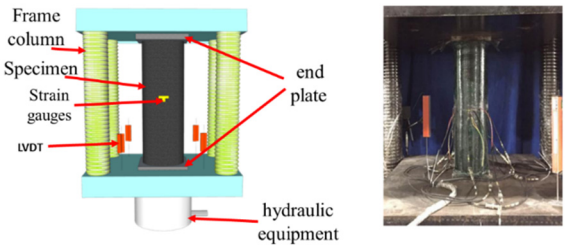

Fig.3 Test setup

3 Test Results and Analysis

3.1 Destroy mode

Figure 4 shows the failure mode of the CFRP-reinforced concrete-filled steel tubular member. During the test, there was a slight compaction of the specimen at the initial stage of loading. When the load reached 76% of the ultimate load, the concrete had a sound, which did not stop. When the load reaches 90%, the lower end of CFRP cracks and produces sound. As the axial deformation increases, the middle part of the CFRP begins to crack, as shown in Fig.4(a) (b). Subsequently, the middle part is completely cracked. When the load reaches 66%, the middle part of the steel pipe is buckled, and the middle and lower part of the CFRP is completely cracked, as shown in Fig.4(c) (d). At the same time, it can be seen from Figure 4 that for the specimens reinforced with circumferential voids, the cracking of CFRP is mostly localized. The author analyzes that the main reason is that the existence of circumferential void defects makes the steel pipe unable to be repaired. Core concrete provides effective restraint. The crushed core concrete could not completely contact the inner wall of the steel pipe, and was randomly distributed in the lower, middle and upper parts of the specimen, so that the steel pipe and the core concrete in this part could play a combined role. The CFRP in this part has the phenomenon of stress concentration, which leads to the final failure mode of local CFRP failure.

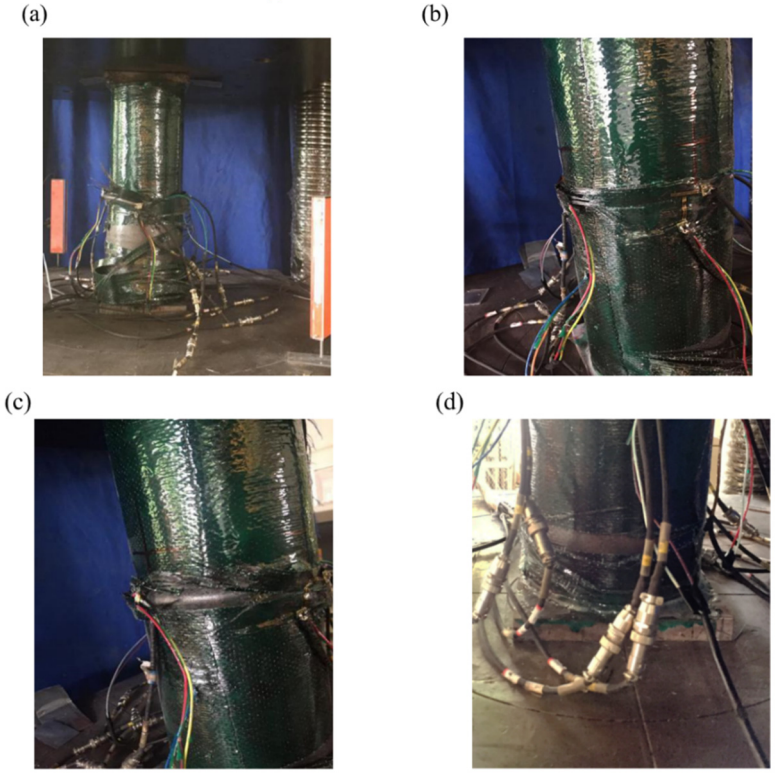

Fig.4 Failure mode of circumferential gap specimen

3.2 Load-displacement curve

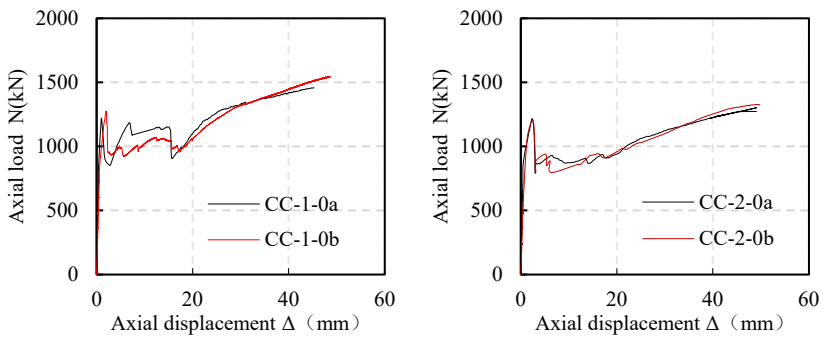

(a) CC-1-0 (b) CC-2-0

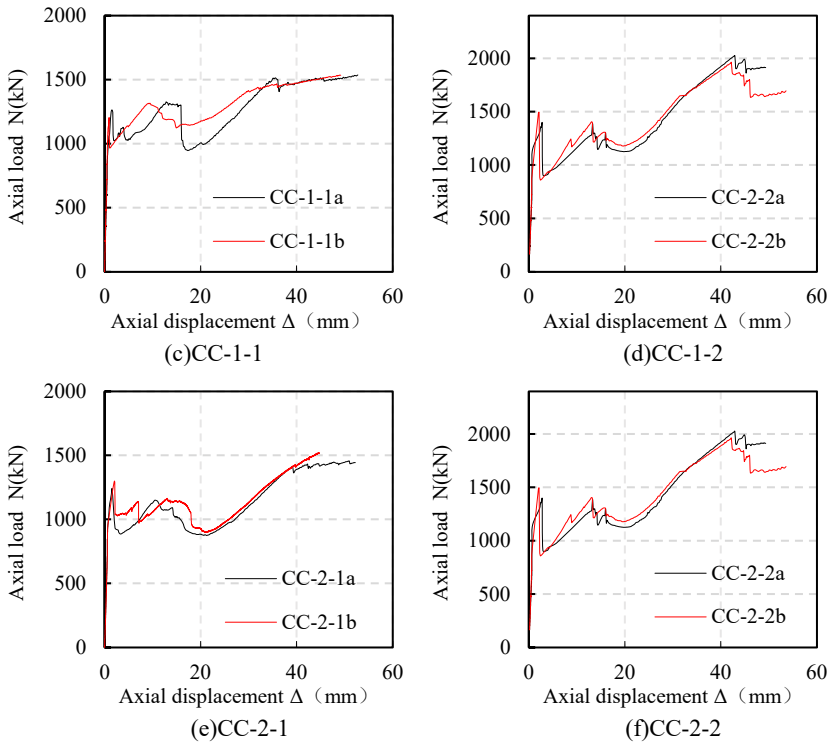

Fig.5 Load(N)-displacement(Δ) curves

It can be seen from Figure 5 that after CFRP reinforcement, after the hoop tensile stress of the outer steel pipe begins to increase, the hoop tensile stress of CFRP gradually increases, and the deformation of the outer steel pipe is delayed when it is constrained by CFRP. In addition, the core concrete Under the double restraint of the outer steel pipe and CFRP, its compressive capacity is increased by 33% compared with that without reinforcement. Especially in the strengthening stage, with the increase of the number of reinforcement layers, the local CFRP has stress concentration, which greatly restrains the local steel pipe. As the amplitude increases, the reinforcement effect becomes more obvious, and the maximum load of the member is obviously greater than its peak load.

The reinforcement effect of CFRP on the specimen with hoop void defect is analyzed by the ultimate bearing capacity. In order to facilitate the comparative analysis, the bearing capacity influence coefficient SI is defined as follows:

$$SI = \frac{N_{ue}}{N_{ue-(co-o)}} \tag{1}$$

Among them, N_{ue} is the bearing capacity of the specimen, and $N_{ue-(co-o)}$ is the average value of the bearing capacity of the specimen without voids.

The 1st and 2nd peak loads were used for the bearing capacity analysis for the unreinforced and reinforced specimens with hoop voiding defects, respectively. The results are shown in Table 6.

3.3 Bearing capacity analysis

Table 6 Comparison of ultimate bearing capacity of specimens

Numbering	layers	Constraint effect coefficient	void rate / χ /%	peak strain / $\mu\varepsilon$	N_{ue} /KN	*SI*
C0-0-0a	-	0.76	-	10857	1722	1
C0-0-0b	-	0.76	-	11569	1779	
CC-1-0a	-	0.76	1.1	5736	1218	0.71
CC-1-0b	-	0.76	1.1	6169	1275	
CC-1-1a	1	1.13	1.1	5586	1256	0.72
CC-1-1b	1	1.13	1.1	6832	1264	
CC-1-2a	2	1.49	1.1	8249	1488	0.85
CC-1-2b	2	1.49	1.1	8191	1486	
CC-2-0a	0	0.76	2.2	5506	1216	0.69
CC-2-0b	0	0.76	2.2	5993	1197	
CC-2-1a	1	1.13	2.2	5808	1237	0.70
CC-2-1b	1	1.13	2.2	6257	1213	
CC-2-2a	2	1.49	2.2	7881	1400	0.82
CC-2-2b	2	1.49	2.2	6478	1495	

Note: For specimens reinforced with CFRP, the confinement effect coefficients are $\xi = \xi_s + \xi_f$, ξ_s , ξ_f and are the confinement effect coefficients of the steel pipe and CFRP

Figure 6 shows the comparison of the influence coefficient of the bearing capacity of the specimens. It can be seen that with the increase of the void ratio, the ultimate bearing capacity of the specimens shows a significant downward trend, decreasing by 29% and 31% respectively. This is mainly due to the difference between the core concrete and the steel pipe. The gap weakens the hoop constraint of the steel pipe to the concrete, so that the steel pipe and the concrete cannot play the combined advantages.

It can be seen from Fig. 6 (b) that the specimen with hoop void defect is strengthened with two layers of CFRP, and the strengthening effect is more obvious, and the SI is significantly improved. When reinforcing one layer, the SI with a void rate of 1.1% is 72%, and the SI with a void rate of 2.2% is 70%; when two layers are strengthened, the SI with a void rate of 1.1% is 85%, and the void rate is 85%. The SI of 2.2% is 82%. After CFRP reinforced the hoop hollow specimen, the bearing capacity was increased by 1.4% when one layer was strengthened, and the bearing capacity was increased by 20% and 19% respectively when two layers were strengthened.

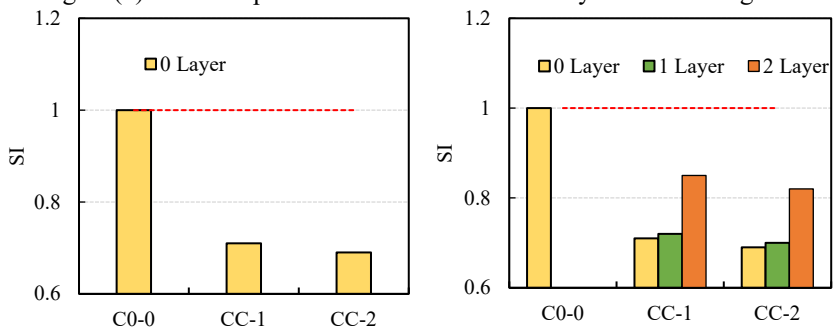

(a) SI comparison of unreinforced specimens (b) SI comparison of CFRP-reinforced annular voids

Fig. 6 Comparison of strength index

3.4 Impact of CFRP Layers

During the test, the specimens with circumferential voiding defects were reinforced with 1 and 2 layers. Figure 7(a) and (b) are divided into 1 and 2 layers of CFRP reinforcement with axial load-axial displacement curves of 1.1% and 2.2% hoop void ratio. It can be seen that there is a certain gap between the steel pipe and the core concrete in the specimen with the hoop void defect, and the combined effect of the two "1+1>2" is greatly weakened. After the core concrete was crushed, the bearing capacity of the specimen dropped sharply, and the CFRP reinforcement could not fully exert its constraining effect. The restraint of CFRP is manifested in delaying the buckling phenomenon of the steel pipe by applying hoop restraint to the steel pipe. After reinforcement with CFRP, the peak load of the specimen has been improved to a certain extent, but the main reinforcement effect is still manifested in the reinforcement stage, and the maximum load exceeds that of the specimen without voids.

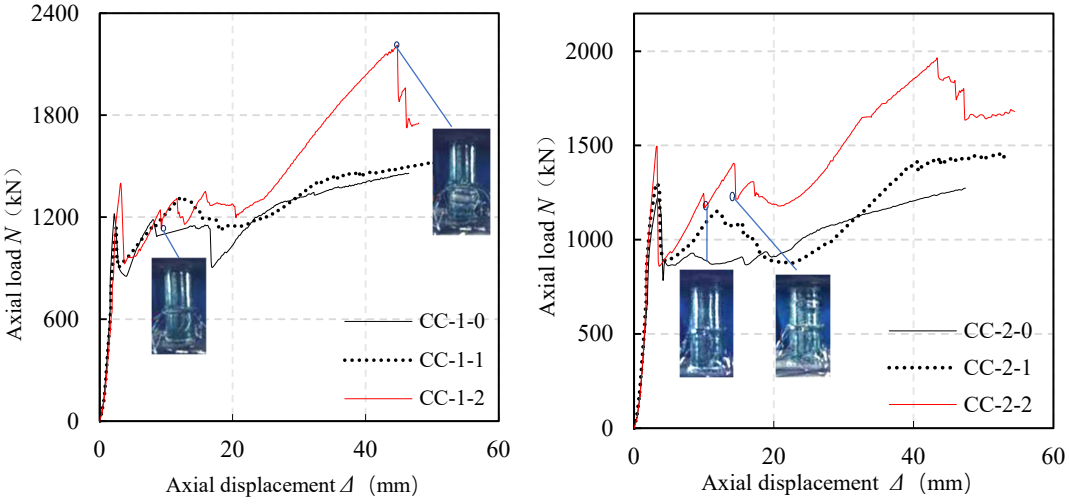

(a) (b)

Fig. 7 Load (N)-Axial Displacement (Δ) curves of CFRP reinforced specimens

Figures 8(a) and (b) show the axial load-axial strain curves of CFRP reinforced with 1-2 layers when the hoop void rate is 1.1% and 2.2%, respectively. It can be seen that for the specimen with annular void defect, the stiffness of the specimen wrapped with CFRP remains basically unchanged in the elastic stage, and the longitudinal strain growth of the specimen is significantly weakened after the elastic-plastic stage, which indicates that the existence of CFRP can delay the specimen. premature buckling.

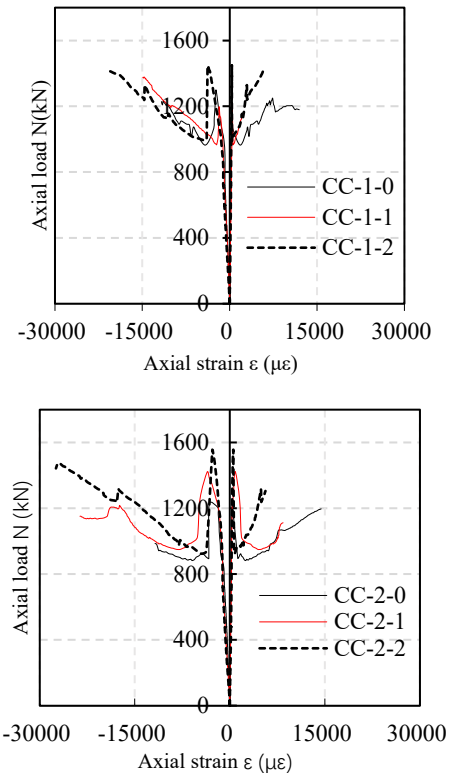

Fig.8 Load (N)-strain ( ) curves of CFRP reinforced specimens

4 Finite Element Analysis

4.1 Model building

Although the mechanical properties of CFRP-reinforced hollow concrete-filled steel tubular short columns under axial compression can be studied intuitively through experiments, it is easily limited by the lack of parameters and insufficient observation content. In this paper, the finite element software (ABAQUS) is used for model analysis to supplement the experimental research, and the model is used as the basis for the analysis of the working mechanism and the parameters. The details of the finite element model are shown in Figure 9. The core concrete, steel pipes, and end plates all use C3D8R solid elements, and CFRP uses S4R shell elements. The contact between the concrete and the upper and lower end plates and the steel pipe adopts surface-to-surface contact, and the contact between the steel pipe and the upper and lower end plates adopts the binding method. Refer to the contact and tangent of the interface normal direction used by Liao[27] in the finite element modeling process. For the bonding-slip method in the direction, the hard contact Hard model is used to define the contact between the steel pipe and the core concrete, and the Coulomb friction Friction model is used to define the contact in the tangential direction. The steel pipe and CFRP use the Tie method to simulate the relationship between the two. Adhesive slip at its interface is not considered. The lower end plate of the member imposes fixed boundary conditions, and the upper end plate constrains all degrees of freedom except the axial displacement, and the axial displacement is applied through the cover plate.

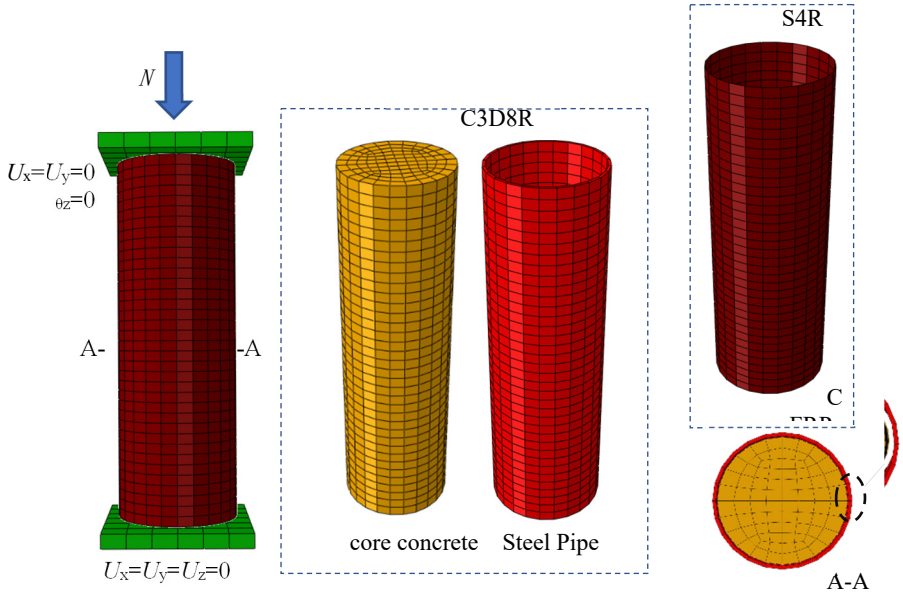

Fig.9 Finite Element Model Details

4.2 model validation

In order to verify the applicability of the model, the axial compressive specimens of CFRP-CFST short columns with circumferential void defects reported by Liao et al[27] and Wang Qingli et al[28] were tested. Finite element simulation check. It can be seen from Table 7 that the simulation results of the finite element method are in good agreement with the experimental results. At the same time, the finite element model is used to simulate the experimental data. It can be seen from the comparison that

the mean value and mean square error of the two are 1.01 and 0.03, respectively. The calculated results of the model are in good agreement with the experimental results, indicating that the model has good calculation accuracy.

Table 7. Comparison of ultimate bearing capacity Nue and Nuc of hollow concrete-filled steel tubular members strengthened by CFRP

serial number	Specimen number	CFRP layers	void rate	N_{ue}(kN)	finite element		Data Sources
					N_{uc}(kN)	N_{uc}/N_{ue}	
1	CC-1-0	-	1.1%-	1581	1557	0.980	Liao[27]
2	CC-2-0	-	2.2%	1489	1531	1.0201	
	average value(u)					0.998	
	mean square error(σ)					0.021	
1	Z0	0	-	889	892	1.003	Wang[28]
2	Z1	1	-	1074	1122	1.045	
3	Z2	2	-	1258	1268	1.008	
	average value(u)					1.0186	
	mean square error(σ)					0.023	
1	CC-1-0	0		1246	1310	1.051	This article
2	CC-1-1	1		1260	1350	1.071	
3	CC-1-2	2		1487	1478	0.994	
4	CC-2-0	0		1206	1292	1.071	
5	CC-2-1	1		1225	1295	1.057	
6	CC-2-2	2		1447	1453	1.004	
	average value(u)					1.019	
	mean square error(σ)					0.031	

4.3 Working mechanism analysis

Taking the annular void rate of 1% as a typical example, the diameter of the steel pipe is 400 mm, the thickness is 9.3 mm, and the length is 1200 mm; the strength of the core concrete is 60 MPa; the strength of the steel pipe is 345 MPa; Plastic flow model[3]; CFRP is hoop reinforcement, the number of reinforcement layers is 3, the thickness of a single layer is 0.17mm, the ultimate tensile strength is 3600MPa, and the elastic modulus is 2.80×105Mpa.

4.3.1 Analysis of the whole process of load and deformation

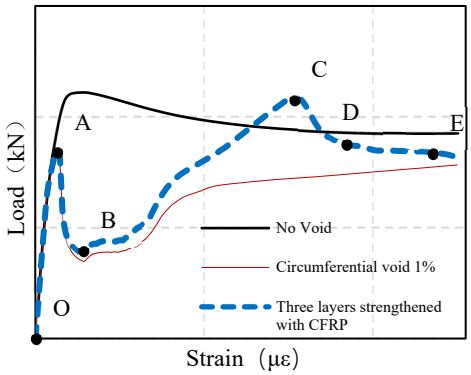

Fig10. Axial load-axial strain relationship curve of typical member

The load-displacement curve of a typical example is shown in Figure 10. It can be seen that the loading process can be divided into the following stages:

(1) Elastic stage (OA section): In the initial stage, both the steel tube and the concrete are in the elastic stage, and there is no interaction between the two due to the existence of void defects.

(2) Descending stage (section AB): Due to the existence of annular voids, the interaction between the steel pipe and the concrete is greatly reduced, and the

bearing capacity drops sharply after the concrete is crushed. The existence of CFRP limits the deformation of the steel pipe, and the existence of voids makes it unable to provide restraint for the concrete. After the concrete is crushed, the bearing capacity drops sharply.

(3) Fluctuation stage (BC section): With the increase of axial displacement, the deformation of the component increases, the steel pipe and the core concrete begin to contact, and the bearing capacity of the component increases, but due to the particularity of the hoop void, the steel pipe and the core concrete are in contact with each other. The core concrete is not completely in contact, only the steel tube in the concave part is in contact with the core concrete. With the increase of the axial displacement, the deformation of the steel pipe is obvious, and the supporting effect of the core concrete on the concave part of the steel pipe is more obvious. At the same time, CFRP still has corresponding constraints on the convexity of the steel pipe, and the bearing capacity fluctuates to a certain extent and gradually increases.

(4) Slump stage (CD section): The steel pipe in the concave part and the core concrete support each other, and the CFRP constrains the convex deformation of the steel pipe. With the increase of the convex deformation of the steel pipe, the local CFRP reaches the ultimate tensile strength. fracture, resulting in a sudden drop in bearing capacity.

(5) Stable stage (DE section): As the deformation increases, the bearing capacity gradually becomes flat.

4.3.2 Stress-Strain Analysis

(1) Stress analysis of core concrete

Figure 11 shows the longitudinal stress field distribution of the mid-section of the core concrete at each characteristic point. In the initial stage, the steel pipe and the core concrete are independently stressed, and the longitudinal stress distribution is basically uniform. At point B, the bearing capacity decreases significantly, and the longitudinal direction of the core concrete decreases from the inward to the core. For unreinforced members, the core concrete lacks the hoop restraint of the steel tube, and its longitudinal stress is lower than that of the non-voided members.

In the BC stage, the crushed core concrete starts to come into contact with the steel pipe. CFRP limits the deformation of the steel pipe, resulting in an increase in the hoop restraint of the core concrete, the increase in the compressive strength of the core concrete, and the gradual increase in its stress value. At point C, the CFRP reaches the tensile strength and breaks. The core concrete bears the greatest hoop restraint, and its stress value increases significantly.

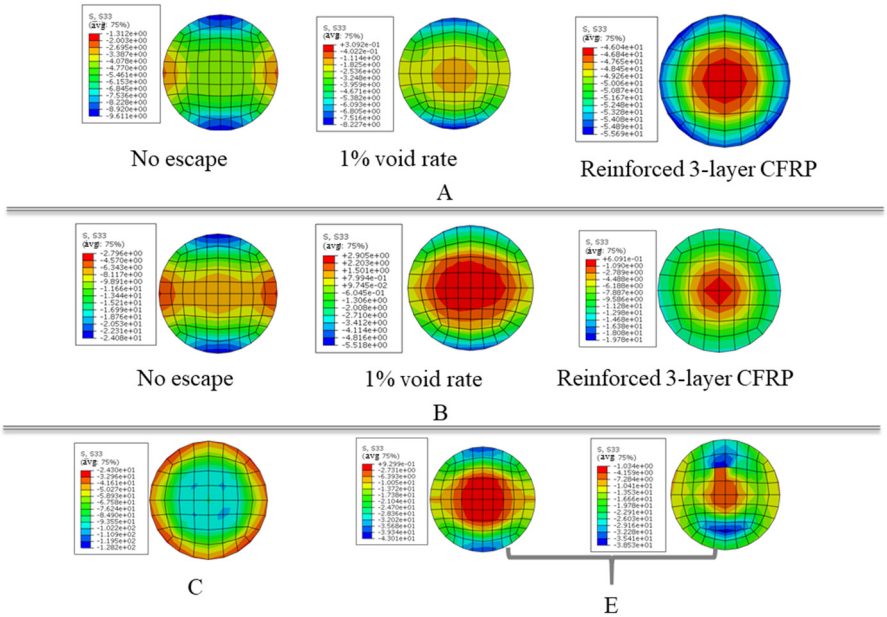

Fig11. Cloud map of stress distribution in core concrete mid-section at each feature point

(2)Stress Analysis of Steel Pipes

Figure 12 shows the Mises stress distribution cloud map of the steel pipe at each characteristic point. It can be seen from the figure that at point A, the overall stress of the steel pipe is relatively uniform, and the end stress is large, which is consistent with the failure process of the component. At point C, CFRP has the largest circumferential constraint on the steel pipe, and the stress at the upper and lower ends of the steel pipe is relatively concentrated.

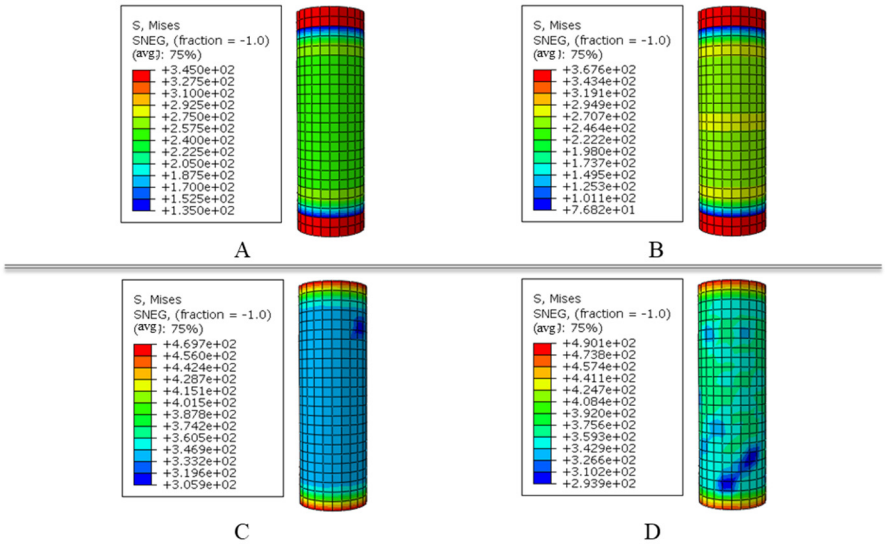

Fig12. Mises stress distribution cloud map of steel pipe under each feature point

(3)Stress Analysis of CFRP

Figure 13 is the cloud diagram of the longitudinal stress field distribution of CFRP at each characteristic point. It can be seen from the figure that the restraint effect of CFRP on the steel pipe is not obvious at the initial stage, and the overall force of CFRP is relatively uniform; after point B, the core concrete is in contact with the steel pipe. When the constraint increases, the CFRP stress value increases significantly. At point C, CFRP constrains the steel pipe the most, it reaches the ultimate tensile strength, and CFRP breaks. In the CD stage, the component area is flat, and the CFRP gradually fails.

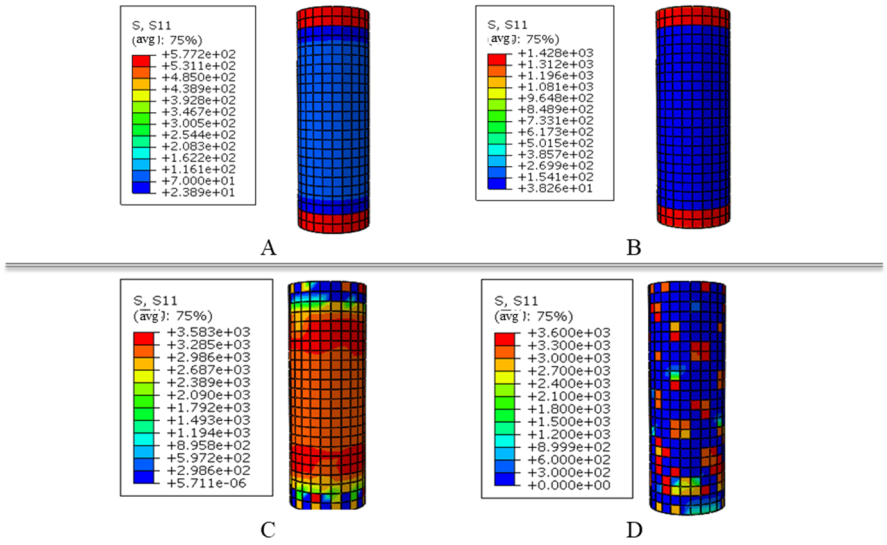

Fig13. Cloud map of longitudinal stress distribution of CFRP under each feature point

5 In conclusion

In order to study the mechanical properties of CFRP-reinforced concrete-filled steel tubular (CFST) members with circumferential void defects, the axial compression test of CFRP-reinforced CFST short columns with circumferential void defects was carried out. In addition, an effective numerical model was established using ABAQUS software. , and supplemented the analysis of the whole process of component failure. The main conclusions of this study are as follows:

(1) After the specimen with hoop voiding defect reaches its ultimate load, the core concrete is crushed and the load drops sharply. As the steel pipe and the core concrete begin to contact, the hoop tensile stress of the steel pipe gradually increases, and the load shows an upward trend again. . With the increase of the void ratio, the ultimate bearing capacity and the corresponding displacement decrease, and the deformation capacity of the specimen is weakened to a certain extent.

(2) After using CFRP to reinforce the hollow specimen, the peak load and the corresponding displacement of the peak point are improved, and the deformation capacity of the specimen is enhanced. When reinforcing 1 layer, the bearing capacity is increased by 1.4%. When reinforced with 2 layers, the bearing capacity is increased by 19-20%. It can be seen from the SI coefficient analysis that CFRP can effectively limit the deformation of the steel pipe, provide better hoop restraint for the concrete, and greatly improve the ultimate bearing capacity and deformation capacity of the specimen.

(3) The finite element software was used to simulate the previous researchers' experiments and the axial compression test conducted this time, and the model calculation results were compared with the test results. The results show that the finite element simulation calculation curve is in good agreement with the test curve. Well, the established model has high reliability and accuracy.

(4) The existence of hoop voids greatly reduces the confinement effect of steel pipes on concrete, making it impossible to give full play to the combined advantages of the two. The use of CFRP reinforcement did not make up for the delay in the contact between the steel tube and the core concrete caused by the hoop void defect. Before the peak load, the contact stress between the steel tube and the concrete is basically zero. For the components with hoop void defect, CFRP has a good constraining effect in the later strengthening stage, and the contact stress between the steel tube and the core concrete is obviously increased.

Author Introduction:

Binglun Chen, Research direction: Solid mechanics, combined with material interface damage and fracture, Email: 1043872577@qq.com.

Zhishuo Yang, Research direction: Building Materials and Structures, Email: chengbinglun@163.com.

References

1. ZHONG Shantong. Research and application of unified theory of concrete filled steel tube[M].Beijing: Tsinghua Press,2006.
2. Cai Shaohuai.Modern concrete filled steel tubular structure (Revised Edition)[M].Beijing: People's Communications Press,2007.
3. HAN lin hai.Concrete filled steel tubular structures:theory and practice[M].3rd ed.Beijing:Science Press,2016:1-12.
4. Road and Bridge Test Research Institute, Highway Planning, Survey and Design Institute, Sichuan Provincial Department of Communications. 2009(a). Test report on the concrete density of steel tubes of the main bridge of the Jinma River Bridge on the extension line of Guanghua Avenue and the quality of the welds.[R].2009,9.1.
5. WANG Wei. Study on void mechanism of concrete filled steel tube[D].Chongqing: ChongQing JiaoTong university,2008.
6. TU Guangya.Sparation effects on mechanical behavior of concrete filled steel tubular arch bridge [D].Chang sha:Hunan University,2008:32-69.
7. Feng Zhi, Wang Jianjun, Han Yu, etc. Prevention of debonding and voiding of CFST arch ribs during construction [J].Highway, 2015,60(12):126-129.
8. LIAO F Y,HAN L H,HE S H.Behavior of CFST short column and beam with initial concrete imperfection:Experiments[J].Journal of Constructional Steel Research,2011,67(12):1922-1935.
9. SUN guoshuai,YU Tiehan,DONG Songyuan.et al.Summary of the development and research on concrete filled CFRP-Steel tubular structure[J].Industrial Construction,2007,37(Suppl1):575-578.
10. BELL T,DARBY A,DENTON S.Research issues related to the appropriate use of FRP in concrete structures[J].Construction and Building Materials,2009,23(4):1521-1528.
11. Kabir M Z, Nazari A. Enhancing Ultimate Compressive Strength of Notch Embedded Steel Cylinders Using Overwrap CFRP Patch [J]. Applied Composite Materials, 2011, 19(3-4): 723-738.
12. Wang H, Wu G, Jiang J. Fatigue Behavior of Cracked Steel Plates Strengthened with Different CFRP Systems and Configurations [J]. Journal of Composites for Construction, 2016, 20(3): 04015078
13. Gu Wei, Zhao Yinghua, Shang Dongwei. Bearing capacity analysis of CFRP-CFST short columns under axial compression[J]. Engineering Mechanics, 2006, 23(1): 149-154.
14. Sundarraja M C, Sivasankar S. Axial behavior of HSS tubular sections strengthened by CFRPstrips:an experimental investigation[J]. Science and Engineering of Composite Materials, 2012, 19(2): 159-168.
15. Prabhu G G, Sundarraja M C, Kim Y Y. Compressive behavior of circular CFST columns externally reinforced using CFRP composites. Thin-Walled Structures, 2015, 87: 139-148.
16. Wang Qingli, Zhang Yongdan, Xie Guangpeng, Yu Shuqin. Bias test of circular section CFRP-concrete-filled steel tubular column [J]. Journal of Shenyang Jianzhu University (Natural Science Edition), 2005, 21(5): 425-429.
17. Wang Chunyu. Experimental Research on Mechanical Properties of CFRP-reinforced Eccentrically Compressed Round Steel Tube Columns [D]. Hefei: Hefei University of Technology, 2017.
18. Ding Lei. The effect of slenderness ratio on the axial compression performance of CFRP-reinforced steel-concrete columns [D]. Hefei: Hefei University of Technology, 2017.
19. Qin P, Xiao Y. Behavior of CFRP Confined Circular Concrete-Filled Steel Tube Columns[C]. Proceedings of the 10th International Conference on Advances in steel concretes composite and hybrid structures, Singapore, 2012: 597-604.
20. Tao Z, Han L H, Zhuang J P. Cyclic performance of fire-damaged concrete-filled steel tubular beam-columns repaired with CFRP wraps[J]. Journal of Constructional Steel Research, 2008, 64(1): 37-50.
21. Zhang Daijun, Tang Bangming, Bao Jianwen, et al. Study on natural aging properties of T700/5288 carbon fiber composites in Hainan [J]. Materials Engineering, 2012, 11: 31-34.
22. National Standard of the People's Republic of China (GB/T228-2002). Greenhouse Tensile Test Method for Metal Materials. General Administration of Quality Supervision, Inspection and Quarantine [S].

Beijing: China Planning Press, 2002.

23. National Standard of the People's Republic of China GB/T50081-2002. Standard for test methods for mechanical properties of ordinary concrete [S]. Beijing: China Construction Industry Press, 2003.
24. National Standard of the People's Republic of China GB/T3354-2014. Test Methods for Tensile Properties of Oriented Fiber Reinforced Polymer Matrix Composites [S]. Beijing: China Standard Press, 2014.
25. Han Linhai. Concrete-filled steel tubular structures—theory and practice (Second Edition) [M]. Beijing: Science Press, 2007
26. Yue Qingrui, Yang Yongxin. Technical specification for repairing concrete structures reinforced with carbon fiber sheets [J]. Building Structure, 2003, 6.
27. Liao FY, Han LH, Tao Z. Behavior of CFST stub columns with initial concrete imperfection：Analysis and calculations[J]. Thin-walled Structures, 2013, 70(13): 57-69.
28. Wang Qingli, Li Ning, Han Fo, Zhu Hefei. Experimental study on CFRP-CFST axial compression members [J]. Journal of Shenyang Jianzhu University (Natural Science Edition), 2006, 22(5): 709-712.
29. Peng Zhiqiang. Research on the mechanical properties of stainless steel tubular concrete members with void defects under partial tension [D]. Fuzhou: Fujian Agriculture and Forestry University, 2013.
30. Liao FY, Han LH, He SH. Behavior of CFST short column and beam with initial concrete imperfection: Experiments [J]. Journal of Constructional Steel Research. 2011, 67(12): 1922-1935.